Published in final edited form as:
Mol Pharm. 2010 February 1; 7(1): 3. doi:10.1021/mp900116r.

Delivery of Stem Cells to Porcine Arterial Wall with Echogenic Liposomes Conjugated to Antibodies against CD34 and Intercellular Adhesion Molecule-1

Stephanie M. Herbst[1,2], **Melvin E. Klegerman**[1], **Hyunggun Kim**[1], **Jiangbo Qu**, **Harnath Shelat**[1,2], **Michael Wassler**[1,2], **Melanie R. Moody**[1], **Chen-Min Yang**[1,2], **Xinyi Ge**[2], **Yuejiao Zou**[1], **Jonathan A. Kopechek**[4], **Fred J. Clubb**[2,3], **Duane C. Kraemer**[3], **Shaoling Huang**[1], **Christy K. Holland**[4], **David D. McPherson**[1], and **Yong-Jian Geng**[1,2,*,1]

[1] Division of Cardiology, Department of Internal Medicine, University of Texas Health Science Center at Houston, Houston, TX

[2] Texas Heart Institute, Houston, TX

[3] Colleges of Veterinary Medicine and Biomedical Sciences, Texas A&M University, College Station, TX

[4] Department of Biomedical Engineering, University of Cincinnati, Cincinnati, OH

Abstract

In atherosclerosis, the loss of vascular stem cells via apoptosis impairs the capacity of the vascular wall to repair or regenerate the tissue damaged by atherogenic factors. Recruitment of exogenous stem cells to the plaque tissue may repopulate vascular cells and help repair the arterial tissue. Ultrasound-enhanced liposomal targeting may provide a feasible method for stem cell delivery into atheroma. Bifunctional echogenic immunoliposomes (BF-ELIP) were generated by covalently coupling two antibodies to liposomes; the first one specific for CD34 antigens on the surface of stem cells and the second directed against the intercellular adhesion molecule-1 (ICAM-1) antigens on the inflammatory endothelium covering atheroma. $CD34^+$ stem cells from adult bone marrow were incubated on the ICAM-1-expressing endothelium of the aorta of swine fed high cholesterol diets, which was preloaded with BF-ELIP. Significantly increased stem cell adherence and penetration were detected, in particular in the aortic segments treated with 1 MHz low-amplitude continuous wave ultrasound. Fluorescence and scanning electron microscopy confirmed the presence of BF-ELIP-bound $CD34^+$ cells in the intimal compartment of the atheromatous arterial wall. Ultrasound treatment increased the number of endothelial cell progenitors migrating into the intima. Thus, under ultrasound enhancement, BF-ELIP bound $CD34^+$ stem cells selectively bind to the ICAM-1 expressing endothelium of atherosclerotic lesions.

Keywords

Artery; Atherosclerosis; Stem Cell; Echogenic liposomes; Ultrasound

* Correspondence: Yong-Jian Geng, MD, PhD, Professor and Director, The Center of Cardiovascular Biology and Atherosclerosis, Department of Internal Medicine, The University of Texas Medical School at Houston, 6431 Fannin Street, MSB 1.246, Houston, TX 77030, USA. Telephone: 713-500-6071, Fax: 713-500-0577 yong-jian.geng@uth.tmc.edu.

Introduction

Advanced atherosclerotic plaques are structurally unstable and may disrupt suddenly.1 Consequently, the ruptured plaque releases thrombogenic materials that can cause blood coagulation, and eventually occlude the artery. This can lead to ischemia or infarction of the distal tissue or organ. Structurally, a plaque prone to rupture is characterized by increased accumulation of lipids and inflammatory cells and smooth muscle cell death, particularly in the fibrotic cap and shoulder regions of the plaque.[1] During atherogenesis, endothelial cells are activated and they express adhesion proteins at higher levels, such as intercellular adhesion molecule-1 (ICAM-1) and vascular cell adhesion molecule-1 (VCAM-1).[2, 3] These molecules facilitate leukocyte adherence and transmigration into the intima of the arterial wall, and induce inflammation. Usually, ICAM-1 expression persists, while VCAM-1 expression declines as the atheroma progresses. Thus, ICAM-1 plays a key role in the leukocyte adhesion and transmigration.

Vascular stem cells contribute to tissue repair and regeneration. In atherosclerosis, however, the capacity of tissue stem cell survival, growth and differentiation is considerably compromised by various atherogenic risk factors, such as hypercholesterolemia [4, 5], diabetes [6, 7], aging[8] and inflammation.[9] Hence, transplantation of exogenous healthy stem cells offers a novel therapeutic strategy for healing of vascular tissue and prevention of plaque rupture. Recent experimental animal research and clinical trials have demonstrated therapeutic potential of multipotent stem cells for atherosclerosis-associated heart diseases.[10] In atherosclerotic mice, intravenous administration of bone-marrow-derived stem cells may attenuate the progression of atherosclerosis. However, the potential therapeutic effects of stem cells introduced directly into atherosclerotic lesions to assess their ability to differentiate into beneficial cell types and aid in plaque stability are currently unknown.

Controlled delivery systems of drugs or other therapeutic agents using biodegradable materials, such as liposomes offer many advantages over traditional methods of drug delivery, including the effectiveness of antibody-loading and targeting to appropriate cell types.11 Optimization of liposomal delivery methods can eliminate side effects of drug over-dosing. Liposomal preparations containing specific molar mixtures of lipids are echogenic,[12] which may be useful in biological studies as a means of enhancing intravascular and transvascular mobility of cells. In addition, liposomes may be modified through antibody conjugation in order to target the liposomes to specific tissues or cell types. This introduces the possibility of using liposomes in therapeutic measures through conjugation to cell-specific antibodies. We have developed intrinsically echogenic immunoliposomes (ELIP) as both an ultrasound contrast agent and an ultrasound-triggered controlled release delivery vehicle. ELIP can be bound to various tissue markers by covalent attachment of ligands to the phosphatidylethanolamine head groups, enabling site-specific ultrasound highlighting or delivery of therapeutic agents, including drugs, genes, and bioactive gases. We have utilized ELIP conjugated to monoclonal anti-human ICAM-1 antibodies that cross-react with the porcine antigen to highlight early and mid-stage atheroma in Yucatan miniswine by both transvascular and intravascular ultrasound.[13, 14] The molecular characteristics of the targeted ELIP were also studied, including interaction affinity and binding thermodynamics.15

Ultrasound has the ability to enhance and provide controlled delivery of therapeutics at the target site.16 This methodology, known as sonoporation, can be augmented by small air or gas pockets within the delivery vehicle which nucleate cavitation.[17] Our objective was to develop ELIP that could selectively deliver vascular stem cells to vulnerable atheroma, while enabling controlled release of agents that enhance stem cell penetration and amelioration of the inflammatory environment. To achieve this objective, we produced bifunctional ELIP (BF-ELIP) that would serve as an appropriate delivery vehicle by binding both immobilized

ICAM-1 and $CD34^+$ human peripheral stem cells. We evaluated the ability of 1-MHz low-amplitude continuous wave ultrasound with BF-ELIP to enhance delivery of stem cells into the arterial wall.

Materials and Methods

Isolation of Porcine Bone Marrow Stem Cells

This study was approved by the Animal Care and Use Committee of the University of Texas Health Science Center at Houston. Stem cells were isolated from bone marrow of one adult male Sinclair cross miniswine approximately 2 years of age. The animal was anesthetized and subsequently euthanized by cardiac puncture according to a protocol approved by the institutional animal care committee. Bone marrow from the femur was extracted and transferred immediately to sterile tissue culture conditions. The gelatinous nature of porcine bone marrow allowed stem cells to remain protected from contamination. The marrow matrix was dissected into pieces of less than 0.5 cm and placed into culture medium containing 10% fetal bovine serum (FBS, Atlanta Biologicals) and 1x each of pen-strep (Gibco) and non-essential amino acids (Gibco). Colonies of cells consistent in size and morphology to SCs were noted by day 7-10 following initial culture. Once cells grew to approximately 70% confluence, they were passaged, transfected with GFP through Adenoviral vector (VECTOR INFO), labeled with the fluorochome DAPI, and frozen in liquid nitrogen. Peripheral mononuclear cells were isolated from healthy blood donors or porcine bone marrow aspirated freshly from domestic pigs, and they were separated from red blood cells and granulocytes by Ficoll-Paque density-gradient centrifugation. In brief, heparinized bone marrows were diluted in PBS and layered onto Ficoll-Paque solution (1-1.5:1), and centrifuged at 1500 RPM for 30 min. Mononuclear cells at the middle layer were collected, washed in PBS, and grown in DMEM medium. In some experiments, peripheral blood samples were collected and used for preparation of mononuclear cells. Non-adherent cells and hematopoietic cells were removed during culture and passage, and stem cells were collected for experiments.

ELIP Preparation

ELIP were prepared by the dehydration-lyophilization-rehydration method as described previously.[18] The ELIP composition consisted of egg phosphatidylcholine (PC), dipalmitoylphosphatidylethanolamine (DPPE), dipalmitoylphosphatidylglycerol (DPPG), and cholesterol (Ch). For rhodamine labeling, rhodamineB-DPPE was added at a molar ratio of 0.02. All phospholipids were purchased from Avanti Polar Lipids (Alabaster, AL). The component lipids were dissolved in chloroform and the solvent was allowed to completely evaporate. The resulting lipid film was placed under vacuum for complete drying and then rehydrated with 0.32M D-mannitol. This dispersion was sonicated until an approximate average vesicular diameter of 500 nm was obtained and the sample was frozen at −70 °C. The samples were lyophilized for 24-48 hours.

Liposome-antibody conjugation

For conjugation, ELIP were prepared as described above, substituting 1,2-dipalmitoyl-sn-glycero-3-phosphoethanolamine-N-[4-(*p*-maleimidophenyl) butyrate] (MPB-PE) for PE. A monoclonal antibody (mAb) to human/mouse ICAM-1 and a rabbit polyclonal Ab to human/mouse CD34 (Santa Cruz Biotechnology, Santa Cruz, CA; with 80% nonspecific carrier IgG to provide an optimal initial IgG mass of 2 mg/29 mg ELIP lipid) were reacted with 3-(2-pyridyldithiolpropionic acid)-N-hydroxysuccinimide ester (SPDP) at a SPDP-protein molar ratio of 15:1 for 30 min at room temperature (RT). Protein was separated from unreacted SPDP by gel chromatography on a 50 ml Sephadex G-50 column equilibrated with 0.05 M citrate-phosphate buffer, pH 5.5. Protein fractions were identified (optical absorbance at 280 nm, A_{280}), pooled and concentrated to ≤ 2 ml using Centricon YM-10 centrifugal filter units. The

PDP-protein was reduced in 25 mM dithiothreitol (DTT) for 30 min at RT. The thiolated protein was isolated (G-50 column), equilibrated and eluted with pH 6.7 citrate-phosphate buffer. Protein-containing fractions were pooled and concentrated. The purified thiolated protein was reacted with reconstituted MPB-ELIP (10 mg lipids/ml 0.1 M phosphate buffer, pH 6.62) under argon overnight at RT. ELIP were separated from free protein and low molecular weight products by gel filtration on a 20-ml Sepharose CL-4B column that had been pre-saturated with unconjugated ELIP according to the method of Lasch et al.[19] and equilibrated with 0.02 M phosphate-buffered saline (PBS), pH 7.4. Liposome-containing fractions prior to elution of free IgG, identified by optical absorbance at 440 nm during calibration of the column, were pooled and lyophilized with 0.1M D-mannitol. Conjugation efficiency (CE, in μg Ab/mg lipid) of Ab-ELIP was determined by quantitative immunoblot assay20 relative to a composite curve of IgG-ELIP secondary standards. Ab-ELIP size distribution and number were determined with a Coulter Multisizer 3, fitted with a 20 μm aperture tube, which permits sizing down to 400 nm equivalent spherical diameter.

ELISA evaluation of ELIP-Ab binding

A sandwich ELISA protocol was used to determine Ab-ELIP targeting efficiency for human ICAM-1. Nunc MaxiSorp microtiter plates were coated with 5 μg/ml of a polyclonal anti-human ICAM-1 capture Ab (R&D Systems, Minneapolis, MN) in 0.05 M sodium bicarbonate, pH 9.6, overnight at 4 °C. All incubation volumes were 50 μl/well. One-third of wells were left uncoated for determination of nonspecific binding. After aspirating well contents, all wells were blocked with conjugate buffer (1% bovine serum albumin (BSA) in 0.05 M Tris buffer, pH 8.0, with 0.02% sodium azide) for 1 hour. From this point, all incubations were at 37 °C. Each incubation was followed by aspiration of well contents and washes (3X) with PBS-T (0.02 M phosphate-buffered saline, pH 7.4, with 0.05% Tween 20). All wells were then incubated with 200 ng/ml of recombinant soluble human ICAM-1 in 0.1% BSA/PBS-T diluent for 2 hours. For assay of intact MAb-ELIP, wells were washed with PBS after this incubation and the first wash after the Ab-ELIP incubation was also with PBS. Various dilutions of MAb and MAb-ELIP in PBS were incubated for 1 hour, followed by a 1-hour incubation with 1:1,000 goat anti-mouse IgG-alkaline phosphatase (Bio-Rad Laboratories, Hercules, CA) in conjugate buffer. The substrate incubation consisted of 50 μl of substrate buffer (0.05 M glycine buffer, pH 10.5, with 1.5 mM magnesium chloride) + 50 μl *p*-nitrophenyl phosphate (Sigma Chem. Co.; 4 mg/ml) in substrate buffer per well for 15 minutes. The reaction was stopped with 50 μl 1 M sodium hydroxide per well. The optical absorbance of each well at 405 nm (A_{405}) was measured with a Tecan Safire^2 microplate reader. Net A_{405} was determined by subtracting the absorbance of background wells from that of capture Ab-coated wells. The dissociation constant (K_D) of MAb-ELIP binding to rshICAM-1 was derived as b of $y = a*x/(b + x)$ from a hyperbolic fit of the ELISA data (y = Net A_{405}, x = [Ab]) performed with SigmaPlot (Systat Software Inc, Point Richmond, CA). [Ab] for Ab-EGIL was calculated from the conjugation efficiency. K_D values were corrected for perturbation of equilibrium conditions during the anti-mouse IgG-AP incubation according to the method of Underwood.[15, 21] The targeting efficiency was determined as avidity, which is the product of CE, expressed as number of Ab molecules per liposome, and the K_{assoc}. An avidity $\geq 1\times10^{12}$ M^{-1} $liposome^{-1}$ is considered optimal. Other measures of TE are the K_D expressed as μg lipid/ml and the functional avidity (product of K_{assoc} and number of Ab molecules/liposome binding to immobilized antigen, calculated from ELISA-determined CE relative to IBA-determined CE), which is closely related to ELIP adherence probability.[22]

ELISA for Assessing Stem Cell Binding to Endothelium

Two modified ELISA protocols were employed to demonstrate the ability of BF-ELIP to bind both ICAM-1 and $CD34^+$ cells. First, the ICAM-1 ELISA protocol was carried through the BF-ELIP/PBS incubation step, as described above. After washing (3X in PBS), human

monocytes (3.5×10^5 in 50 μl 1% BSA/PBS diluent) from healthy donors, transfected with the GFP gene as described below, were added to each well and incubated at 37 °C for 1.7 hours. Wells were washed and trypsinized (0.25%, 100 μl) for 5 minutes. The reaction was stopped with an equal volume of soybean trypsin inhibitor (Gibco). Well contents were removed and cells counted in a hemacytometer by phase contrast microscopy. Second, human umbilical vein endothelial cells (HUVEC) were grown to 75% confluence in collagen-coated microplate wells. Prior to the experiment, cells were incubated overnight with tumor necrosis factor α (TNFα) (R&D Systems, Minneapolis, MN; 20 ng/ml) to stimulate expression of ICAM-1. All incubations were in Endothelial Cell Culture Medium (ECCM, Am. Type Culture Collection) at 37 °C in an atmosphere of 5% carbon dioxide/95% air, followed by 3 PBS washes. Initial 2-hour incubation with 4.7×10^7 BF-ELIP/well was followed by human monocytes (3.5×10^5 in 50 μl/well) for 1 hour and by phycoerythrin-labeled anti-CD34 (250X in ECCM; Abcam, Cambridge, MA) for 1 hour. After addition of 150 μl ECCM, fluorescence emission (575 nm, 533 nm excitation) of wells was measured in the Tecan Saphir2 reader.

Calibration of the 1-MHz Continuous Wave Ultrasound System

A 1-MHz ultrasound transducer (Sonitron 1000, Rich-Mar Corp, Inola, OK) which has a 1 cm aperture, was used to expose the ex vivo porcine arteries to ultrasound. This transducer was calibrated to determine the acoustic pressure output and beam characteristics using a 0.5 mm-diameter PVDF needle hydrophone (Precision Acoustics, Dorchester, England). Briefly, calibration measurements were performed in a water-filled 36 cm × 24 cm × 20 cm acrylic tank at room temperature (20 to 23 °C). The Sonitron transducer was submerged using a rigidly supported positioner, and the PVDF needle hydrophone was mounted on a motorized three-axis translation system (Velmex NF90 Series, Velmex Inc, Bloomfield, NY) and aligned with the transducer. The hydrophone was inserted through a 2.0 cm × 3.5 cm slab of acoustic absorber material (Precision Acoustics, Dorchester, England) in order to minimize standing wave interference from the positioner. Hydrophone measurements were digitized using a digital oscilloscope (WaveRunner, LeCroy Corp, Chestnut Ridge, NY) and transferred to a desktop computer. All calibration measurements were automated and controlled with a collection of visual interface programs written in LabVIEW (National Instruments, Austin, TX) on the desktop computer. Using a Sonitron output dial setting of 0.5 W/cm^2 the peak-to-peak pressure amplitude at an axial distance of 5 mm is 0.15 MPa.

Liposomal Targeting of Stem Cells to Aortic Walls under Ultrasound

A porcine model for atherosclerosis was used for this study. Adult Sinclair cross miniswine (N=3) and Yucatan miniswine (N=5) fed high cholesterol diet (2% cholesterol and 15% lard) for 4 weeks were anaesthetized and subsequently euthanized under surgical conditions according to an approved protocol. Immediately after sacrifice, the descending thoracic aorta was removed and placed into ice-cold Dulbecco's PBS (DPBS, Gibco). The thoracic aorta was dissected longitudinally and again cross-sectionally, into pieces of approximately 2 cm^2. Aortal segments (18 total; 6 per liposomal/PBS treatment group, half of which were subjected to ultrasound) were placed endothelial-side-up onto acoustically absorptive rubber. A 0.5 ml aliquot of the liposomal preparation (~ 3.5×10^5 BF-ELIP), with or without rhodamine B-DPPE incorporated into the lipid bilayer, was added to the endothelial surface of the aortal segment and incubated for 5 minutes at 37 °C. DPBS and IgG-ELIP were used as controls. The segment was washed to remove unbound liposomes. Approximately 1.5×10^5 porcine adipose or 3.3×10^5 bone marrow stem cells in a volume of 0.5 ml Dulbecco's MEM or DPBS, respectively, were added and again incubated for 5 minutes at 37 °C. After washing with PBS, one-half of the segments were subjected to 1-MHz continuous wave ultrasound for 30 seconds. The 1-MHz Sonitron transducer was mounted 5 mm above each exposed aorta segment such that the arterial wall was exposed to 0.15 MPa peak-to-peak pressure amplitude (0.18 W/cm^2). The aortic segments were submerged in saline directly on acoustically absorptive rubber to

minimize constructive interference. Following ultrasound treatment, aortal segments were incubated in IMDM (Gibco) in 24-well culture plates for 2 hours at 37 °C, after which time each segment was dissected into 3 pieces. Two pieces were fixed in 4% paraformaldehyde and 3% glutaraldehyde, respectively. The third was snap-frozen in OCT compound on dry ice.

Histopathology

After incubation with ELIP-stem cells, aortic segments were fixed in 4% paraformadehyde, paraffin-embedded, and sectioned at thickness of 6 μm. Routine histopathological analysis was performed by staining of aortic sections with hematoxylin and eosin (H&E) or by Mason-Trichome staining. Stained sections were examined with an upright microscope at low and high power. In some experiments, cryosections were prepared for immunofluorescent or fluorescent microscopical analysis, using an Olympus IX70 inverted fluorescence microscope equipped with a Hamamatsu C4742-95 digital camera. For detection of stem cell adhesion and migration, aortic segments were fixed in 3% glutaraldehyde and analyzed for the presence of stem cells with scanning electron microscopy. Here the aortic tissue was dehydrated in ethanol, in a graded series of 10 min incubations in 70-100% ethanol and scanned using the JEOL JSM-6460 low-vacuum scanning electron microscope (LV SEM mode). The stem cell-ELIP-endothelial cell binding was also visualized by staining with Oil Red O (1%) for 30 min at room temperature.

Statistics

SigmaStat 3.5 (Systat Software Inc, Point Richmond, CA) was utilized for data analysis using a two-tailed student's t-test or a one-way ANOVA method. A P-value of less than 0.05 was considered to be statistically significant. Data are reported as mean ± standard deviation.

Results

Demonstration of BF-ELIP Binding

ICAM-1 binding of the BF-ELIP was verified by a sandwich ICAM-1 ELISA (Fig. 3). Affinity for human rICAM-1 was about 1.0 nM (K_D). The first ELISA protocol demonstrated an ability of BF-ELIP to promote net binding of human monocytes to an ICAM-1 matrix. In the presence of BF-ELIP, more monocytes were recovered from the wells with the ICAM-1 matrix (Fig. 1), which mimics the surface of activated endothelial cells. Compared to those without added BF-ELIP, addition of BF-ELIP increased the mononuclear cell binding (5.07×10^3 /well in BF-ELIP vs. 3.51×10^3 cells/well in controls). There were fewer cells binding to the wells coated with BSA as compared to those with ICAM-1 containing matrix ($p < 0.01$). In the second ELISA protocol, we directly incubated the GFP-transfected human peripheral mononuclear cells in the wells pre-seeded with human endothelial cells (HUVEC) in the presence or absence of BF-ELIP, followed by incubation with anti-CD34-PE. We observed that there was effective BF-ELIP bridging of HUVEC and CD34+ human monocytes by showing enhancement of both phycoerythrin (PE) and GFP fluorescence relative to the control cultures without BF-ELIP (Fig. 2).

BF-ELIP Binding to Human Peripheral CD34+ Mononuclear Cells

Fluorescent microscopy was performed to directly visualize BF-ELIP binding to human CD34 + cells. Incubation of human peripheral mononuclear cells with BF-ELIP led to the appearance of rosettes consisting of mononuclear cells surrounded by attached multiple ELIP (Fig. 3a and 3b). Nuclear counterstaining with DAPI showed all the rosetted cells with single blue-fluorescent nuclei, while small sized ELIP-particles had no DAPI stain. By contrast, in the mononuclear cells incubated with control IgG-ELIP, little ELIP attachment to cells was found (Fig. 3c and 3d). Further analysis of the mononuclear cells binding with BF-ELIP by flow

cytometry revealed that 3-3.5% of the mononuclear cells from peripheral blood were positively labeled with BF-ELIP stained with anti-mouse IgG-PE (Fig. 4). For comparison, we incubated mononuclear cells with control IgG-ELIP, and found that few of the control cells displayed positive signals (Fig. 4a). Thus, the BF-ELIP appeared to be highly specific, since there was virtually no signal in the cells incubated with unconjugated ELIP or IgG-ELIP.

Enhancement of BF-ELIP Binding to Porcine Aortic Endothelium with Ultrasound

Ex vivo experiments were performed to determine whether BF-ELIP can bind to arterial endothelium in large animals. BF-ELIP labeled with rhodamine was incubated on the inner surface of the freshly excised aorta from swine with or without ultrasound at low acoustic output levels. Little fluorescence was detected in the PBS control group (Fig. 5a). However, when the aortic tissue was incubated with BF-ELIP labeled with rhodamine, followed by porcine bone marrow-derived cells (after washing) 5 minutes, they showed BF-ELIP fluorescence on the lumenal surface (Fig. 5a and 5b). The presence of rhodamine fluorescence on the endothelial surface is an indicator of effective binding of BF-ELIP. Ultrasound treatment increased attachment of BF-ELIP-stem cells to the aorta (Fig. 5b) while only minimal fluorescence was seen on the surface of the aorta without ultrasound treatment (Fig. 5c).

To further verify the BF-ELIP associated bone marrow cell binding to the aortic surface, histopathological analysis demonstrated ELIP-aided stem cell attachment to the aortic endothelium. H&E staining verified the BF-ELIP-associated delivery of mononuclear cells to endothelium (Fig. 5d). The ultrasound-enhanced, BF-ELIP associated delivery of stem cells did not appear to cause any morphological changes in the aortic tissue. The endothelial integrity and medial muscle layers remained intact.

BF-ELIP Enhances CD34+ Cell Adherence to Aortic Endothelium

To further confirm the BF-ELIP-labeled stem cell attachment to the aortic tissue, scanning electron microscopy (SEM) was performed. After treatment with or without ultrasound, the aortic surface incubated with BF-ELIP and bone marrow stem cells was scanned using the JEOL JSM-6460 scanning electron microscope in the LV SEM mode. We observed that there were numerous BF-ELIP-stem cells attached on the lumenal surface of aortas (Fig. 6a and 6b), particularly in those segments following ultrasound treatment. Compared to the area with normal endothelium, regions with fatty streaks had greater numbers of cells attached to the surface, and some of these stem cells appeared to penetrate the endothelial layer (Fig. 6b). This supports the ability of ultrasound to enhance attachment and penetration of the BF-ELIP-labeled stem cells to the atheromatous arterial wall.

For further quantification of the ultrasound-enhanced, BF-ELIF-binding bone marrow cell adherence to the aortic surface, *en face* Oil Red O staining was performed (Fig. 7). Oil Red O stains the liposomes on the stem cells adherent to the surface of endothelium. Consistent with the results from the studies with fluorescence and electron microscopy, Oil Red O staining clearly demonstrated that ultrasound treatment enhanced adhesion of BF-ELIP-bound CD34+ cells to the regions of fatty streaks whose endothelial cells have increased ICAM-1 expression. Morphometric quantification of Oil Red O staining indicated that low-amplitude (0.15 MPa peak-to-peak pressure), continuous wave 1-MHz ultrasound treatment increased the BF-ELIP-bound stem cell adhesion more than twofold, compared to those without ultrasound treatment and controls (Fig. 7).

Discussion

This is the first study, to our knowledge, providing evidence that ELIP conjugated to two functionally different antibodies enhance stem cell delivery to the arterial wall. Our discussion

will focus on the benefits of this methodology in directing and enhancing stem cell delivery to target tissues.

These data establish the suitability of BF-ELIP with ultrasound enhancement as stem cell delivery agents. Previous investigations have demonstrated that ELIP are very useful agents that can serve as drug/gene carriers and diagnostic ultrasound imaging contrast agents.[12, 23] When conjugated to specific antibodies, ELIP can be used for tissue or organ-specific targeting. The present study has demonstrated the feasibility of BF-ELIP for stem cell delivery from peripheral blood and bone marrow to target tissues.

In atherosclerosis, the vascular tissue is injured by hypercholesterolemia and inflammation. In response to the injury, large numbers of leukocytes but few vascular stem cells enter the arterial lesions. Resident vascular progenitor cells may die by apoptosis or other mechanisms.[1, 9] Early atheroma lesions develop in the intima of the arteries. Here, the lumenal endothelial layer serves as the entry point for both leukocytes and stem cells to transmigrate into the lesions. Increased expression of adhesion proteins, such as ICAM-1 and VCAM-1, is considered to be a key event that triggers vascular inflammatory cell infiltration.[24] By utilizing this event, this methodology creates a new avenue for delivering CD34+ stem cells to atherosclerotic intimal lesions. Endogenous stem cells adhere to the surface via adhesion proteins before entering the arterial wall. The conjugation of anti-ICAM-1 antibodies to the surface of liposomes allows binding of liposomes to ICAM-1-expressing endothelial cells of atherosclerotic lesions, thereby specifically targeting cells involved in early plaque formation.

In addition, selection of specific types of stem cells can be achieved through liposomal conjugation of antibodies against cell-type specific surface markers. Bone marrow-derived stem cells are characterized by several cell-surface markers, including CD29, CD34, CD44, CD90 and CD133. Double-conjugation of echogenic liposomes to both ICAM-1 and stem-cell-specific surface markers to produce bifunctional echogenic liposomes provides a mechanism to allow binding of stem cells to ICAM-1-expressing endothelial cells. Because pre-incubation of BF-ELIP with stem cells would obscure the liposomal ICAM-1 binding sites, it is necessary to administer the BF-ELIP prior to the stem cells. Subsequent coating of ICAM-1 expressing endothelium with stem cell binding sites has the added advantage of recruiting endogenous stem cells, as well as exogenous cell populations introduced after BF-ELIP administration.

It is generally believed that the stem cell traffic and homing is physiologically regulated by a “homing” receptor and its ligand, such as the CXCR4/stromal derived factor system.[25, 26] Relatively few studies have focused on increasing plaque stability as a means of treating atherosclerosis. As stem cells have the ability to differentiate into multiple cell types, introduction of stem cells into atherosclerotic plaques may result in the production of cell types that are able to stabilize the plaque, such as collagen-producing fibroblasts. In this study, we demonstrated that BF-ELIP selectively binds to CD34 and ICAM-1 could recognize both human peripheral CD34+ mononuclear cells and porcine bone marrow cells and subsequently bridge the cells to aortal endothelium. The recognition and binding seem to be specific, since the control IgG-ELIP did not have such capacity.

This bridging function improves the likelihood that BF-ELIP can enable increased binding of CD34+ cells to atheroma, compared to therapeutic interventions not employing such delivery agents, in which tissue binding of stem cells is entirely dependent upon endogenous cellular mechanisms of increased cell adhesion, involving adhesin-integrin-mediated homing to areas of tissue injury. Because BF-ELIP targets stem cells to endothelial cells via the ICAM-1 mediated adhesion, they may competitively inhibit leukocyte adhesion and therefore reduce

inflammatory cell infiltration into atheroma. This notion is supported by the observation that in the BF-ELIP-loaded area, the majority of cells adherent to endothelium are CD34+ cells.

Exciting work in the field of gene therapy demonstrates enhanced cell transfection with the use of low-intensity ultrasound 28-31. It has been suggested that this increased uptake is due to cavitational effects by ultrasound [32], a theory supported by the finding that inclusion of Albunex® (an imaging contrast agent) as a cavitation nucleation agent enhances ultrasound-induced transfection [33]. Petechial hemorrhage and microvascular leakage in the myocardium have also been demonstrated as a result of myocardial contrast imaging at 1.7 MHz in rats 34. The interaction of ultrasound with the encapsulated gas within the BF-ELIP potentially enhances the adhesion to vascular endothelium via radiation force or shear stress mechanisms.

Evidence for clinically relevant sonoporation-enhanced BF-ELIP bridging was provided in the ex vivo porcine aortic segments. Oil Red O staining identified the presence of liposomes on the surface of the aorta. Utilizing Oil Red O as an indicator, we confirmed that ultrasound treatment increased the binding of BF-ELIP-CD34+ stem cell complexes to the aortic endothelial surface, relative to IgG-ELIP controls. This suggests that the aortic surface adherence was mediated by ICAM-1 binding. Although this study was performed on ex vivo tissues under static incubation conditions and may not represent the in vivo situation found in the arteries with blood flow, the ability of BF-ELIP to adhere to lumenal surfaces under simulated physiologic flow conditions[35] and in vivo [13,14,36] has been well established. Other factors besides blood flow that may influence the outcomes of the BF-ELIP guided stem cell delivery include the ratio of BF-ELIP to stem cells and ultrasound energy. In vivo studies, presently underway, will establish whether enhancement of stem cell homing to endothelium is a consistent effect of this liposomal agent used in conjunction with sonoporation.

As we have previously demonstrated that ELIP can be efficiently loaded with various therapeutic agents, followed by ultrasound-induced controlled release,[16, 23, 27] BF-ELIP show additional promise as a platform technology for optimization of experimental therapeutic protocols involving concurrent delivery of drugs and genes to enhance endothelial penetration and survival of stem cells.

Conclusion

The current study reports a novel strategy to use BF-ELIP to deliver CD34 positive stem cells directly to atheroma with active expression of adhesion proteins. Our data clearly demonstrate that under the ultrasound enhancement, BF-ELIP can selectively bind peripheral and bone marrow-derived CD34+ cells and provide targeted delivery to vascular endothelium under controlled in vitro conditions. This novel methodology for stem cell delivery provides a basis for new strategies to improve stem cell therapy for cardiovascular diseases.

Acknowledgments

This work was supported in part by the National Institutes of Health (R01 HL69509 Geng, HL74002 McPherson, HL059586 McPherson, and NS047603 Holland) and the Department of Defense (DREAM/T5 program, Geng).

References

1. Libby P, Geng YJ, Sukhova GK, Simon DI, Lee RT. Molecular Determinants of Atherosclerotic Plaque Vulnerability. Ann N Y Acad Sci 1997;811:134–42. discussion 142-5. [PubMed: 9186592]
2. Boyle JJ. Macrophage Activation in Atherosclerosis: Pathogenesis and Pharmacology of Plaque Rupture. Curr Vasc Pharmacol 2005;3:63–8. [PubMed: 15638783]

3. Schwartz RS, Bayes-Genis A, Lesser JR, Sangiorgi M, Henry TD, Conover CA. Detecting Vulnerable Plaque Using Peripheral Blood: Inflammatory and Cellular Markers. J Interv Cardiol 2003;16:231–42. [PubMed: 12800402]
4. Chen JZ, Zhang FR, Tao QM, Wang XX, Zhu JH. Number and Activity of Endothelial Progenitor Cells from Peripheral Blood in Patients with Hypercholesterolaemia. Clin Sci (Lond) 2004;107:273–80. [PubMed: 15099190]
5. Xu Y, Arai H, Murayama T, Kita T, Yokode M. Hypercholesterolemia Contributes to the Development of Atherosclerosis and Vascular Remodeling by Recruiting Bone Marrow-Derived Cells in Cuff-Induced Vascular Injury. Biochem Biophys Res Commun 2007;363:782–7. [PubMed: 17897625]
6. Fadini GP, Sartore S, Albiero M, Baesso I, Murphy E, Menegolo M, Grego F, Vigili de Kreutzenberg S, Tiengo A, Agostini C, Avogaro A. Number and Function of Endothelial Progenitor Cells as a Marker of Severity for Diabetic Vasculopathy. Arterioscler Thromb Vasc Biol 2006;26:2140–6. [PubMed: 16857948]
7. Kusuyama T, Omura T, Nishiya D, Enomoto S, Matsumoto R, Takeuchi K, Yoshikawa J, Yoshiyama M. Effects of Treatment for Diabetes Mellitus on Circulating Vascular Progenitor Cells. J Pharmacol Sci 2006;102:96–102. [PubMed: 16990702]
8. Rauscher FM, Goldschmidt-Clermont PJ, Davis BH, Wang T, Gregg D, Ramaswami P, Pippen AM, Annex BH, Dong C, Taylor DA. Aging, Progenitor Cell Exhaustion, and Atherosclerosis. Circulation 2003;108:457–63. [PubMed: 12860902]
9. Geng YJ. Molecular Mechanisms for Cardiovascular Stem Cell Apoptosis and Growth in the Hearts with Atherosclerotic Coronary Disease and Ischemic Heart Failure. Ann N Y Acad Sci 2003;1010:687–97. [PubMed: 15033813]
10. Yoon YS, Wecker A, Heyd L, Park JS, Tkebuchava T, Kusano K, Hanley A, Scadova H, Qin G, Cha DH, Johnson KL, Aikawa R, Asahara T, Losordo DW. Clonally Expanded Novel Multipotent Stem Cells from Human Bone Marrow Regenerate Myocardium after Myocardial Infarction. J Clin Invest 2005;115:326–38. [PubMed: 15690083]
11. Schiffelers RM, Koning GA, ten Hagen TL, Fens MH, Schraa AJ, Janssen AP, Kok RJ, Molema G, Storm G. Anti-Tumor Efficacy of Tumor Vasculature-Targeted Liposomal Doxorubicin. J Control Release 2003;91:115–22. [PubMed: 12932643]
12. Alkan-Onyuksel H, Demos SM, Lanza GM, Vonesh MJ, Klegerman ME, Kane BJ, Kuszak J, McPherson DD. Development of Inherently Echogenic Liposomes as an Ultrasonic Contrast Agent. J Pharmaceutical Sciences 1996;85:486–490.
13. Demos SM, Alkan-Onyuksel H, Kane BJ, Ramani K, Nagaraj A, Greene R, Klegerman M, McPherson DD. In Vivo Targeting of Acoustically Reflective Liposomes for Intravascular and Transvascular Ultrasonic Enhancement. J Am Coll Cardiol 1999;33:867–75. [PubMed: 10080492]
14. Hamilton AJ, Huang SL, Warnick D, Rabbat M, Kane B, Nagaraj A, Klegerman M, McPherson DD. Intravascular Ultrasound Molecular Imaging of Atheroma Components in Vivo. J Am Coll Cardiol 2004;43:453–460. [PubMed: 15013130]
15. Klegerman ME, Huang S, Parikh D, Martinez J, Demos SM, Onyuksel HA, McPherson DD. Lipid Contribution to the Affinity of Antigen Association with Specific Antibodies Conjugated to Liposomes. Biochim Biophys Acta 2007;1768:1703–16. [PubMed: 17509522]
16. Tiukinhoy-Laing SD, Huang S, Klegerman M, Holland CK, McPherson DD. Ultrasound-Facilitated Thrombolysis Using Tissue-Plasminogen Activator-Loaded Echogenic Liposomes. Thromb Res 2007;119:777–84. [PubMed: 16887172]
17. Huang SL, MacDonald RC. Acoustically Active Liposomes for Drug Encapsulation and Ultrasound-Triggered Release. Biochimica et Biophysica Acta - Biomembranes 2004;1665:134–141.
18. Huang SL, Hamilton AJ, Nagaraj A, Tiukinhoy SD, Klegerman ME, McPherson DD, Macdonald RC. Improving Ultrasound Reflectivity and Stability of Echogenic Liposomal Dispersions for Use as Targeted Ultrasound Contrast Agents. Journal of Pharmaceutical Sciences 2001;90:1917–1926. [PubMed: 11745750]
19. Lasche, J.; Weissig, V.; Brandl, M. Preparation of liposomes.. In: Torchilin, VP.; Weissig, V., editors. Liposomes. 2nd ed.. Oxford University Press; New York, NY: 2003. p. 24-25.

20. Klegerman ME, Hamilton AJ, Huang SL, Tiukinhoy SD, Khan AA, MacDonald RC, McPherson DD. Quantitative Immunoblot Assay for Assessment of Liposomal Antibody Conjugation Efficiency. Anal Biochem 2002;300:46–52. [PubMed: 11743691]
21. Underwood PA. Problems and Pitfalls with Measurement of Antibody Affinity Using Solid Phase Binding in the ELISA. J Immunol Methods 1993;164:119–30. [PubMed: 8360501]
22. Klegerman ME, Zou Y, McPherson DD. Fibrin Targeting of Echogenic Liposomes with Inactivated Tissue Plasminogen Activator. J Liposome Res 2008;18:95–112. [PubMed: 18569446]
23. Huang SL, McPherson DD, Macdonald RC. A Method to Co-Encapsulate Gas and Drugs in Liposomes for Ultrasound-Controlled Drug Delivery. Ultrasound Med Biol 2008;34:1272–80. [PubMed: 18407399]
24. Galkina E, Ley K. Vascular Adhesion Molecules in Atherosclerosis. Arterioscler Thromb Vasc Biol 2007;27:2292–301. [PubMed: 17673705]
25. Haider H, Jiang S, Idris NM, Ashraf M. IGF-1-Overexpressing Mesenchymal Stem Cells Accelerate Bone Marrow Stem Cell Mobilization Via Paracrine Activation of SDF-1alpha/CXCR4 Signaling to Promote Myocardial Repair. Circ Res 2008;103:1300–8. [PubMed: 18948617]
26. Marquez-Curtis LA, Turner AR, Larratt LM, Letcher B, Lee SF, Janowska-Wieczorek A. CD34+ Cell Responsiveness to Stromal Cell-Derived Factor-1alpha Underlies Rate of Engraftment after Peripheral Blood Stem Cell Transplantation. Transfusion 2009;49:161–9. [PubMed: 18954402]
27. Tiukinhoy SD, Khan AA, Huang S, Klegerman ME, MacDonald RC, McPherson DD. Novel Echogenic Drug-Immunoliposomes for Drug Delivery. Invest Radiol 2004;39:104–10. [PubMed: 14734925]
28. Kim HJ, Greenleaf JF, Kinnick RR, Bronk JT, Bolander ME. Ultrasound-Mediated Transfection of Mammalian Cells. Hum Gene Ther 1996;7:1339–46. [PubMed: 8818721]
29. Huber PE, Pfisterer P. In Vitro and in Vivo Transfection of Plasmid DNA in the Dunning Prostate Tumor R3327-AT1 Is Enhanced by Focused Ultrasound. Gene Ther 2000;7:1516–25. [PubMed: 11001372]
30. Chen S, Shohet RV, Bekeredjian R, Frenkel P, Grayburn PA. Optimization of Ultrasound Parameters for Cardiac Gene Delivery of Adenoviral or Plasmid Deoxyribonucleic Acid by Ultrasound-Targeted Microbubble Destruction. J Am Coll Cardiol 2003;42:301–8. [PubMed: 12875768]
31. Chen S, Ding JH, Bekeredjian R, Yang BZ, Shohet RV, Johnston SA, Hohmeier HE, Newgard CB, Grayburn PA. Efficient Gene Delivery to Pancreatic Islets with Ultrasonic Microbubble Destruction Technology. Proc Natl Acad Sci U S A 2006;103:8469–74. [PubMed: 16709667]
32. Koch S, Pohl P, Cobet U, Rainov NG. Ultrasound Enhancement of Liposome-Mediated Cell Transfection Is Caused by Cavitation Effects. Ultrasound Med Biol 2000;26:897–903. [PubMed: 10942837]
33. Greenleaf WJ, Bolander ME, Sarkar G, Goldring MB, Greenleaf JF. Artificial Cavitation Nuclei Significantly Enhance Acoustically Induced Cell Transfection. Ultrasound Med Biol 1998;24:587–95. [PubMed: 9651968]
34. Li P, Cao LQ, Dou CY, Armstrong WF, Miller D. Impact of Myocardial Contrast Echocardiography on Vascular Permeability: An in Vivo Dose Response Study of Delivery Mode, Pressure Amplitude and Contrast Dose. Ultrasound Med Biol 2003;29:1341–9. [PubMed: 14553812]
35. Demos SM, Dagar S, Klegerman M, Nagaraj A, McPherson DD, Onyuksel H. In Vitro Targeting of Acoustically Reflective Immunoliposomes to Fibrin under Various Flow Conditions. J Drug Target 1998;5:507–18. [PubMed: 9783681]
36. Hamilton A, Huang SL, Warnick D, Stein A, Rabbat M, Madhav T, Kane B, Nagaraj A, Klegerman M, MacDonald R, McPherson D. Left Ventricular Thrombus Enhancement after Intravenous Injection of Echogenic Immunoliposomes: Studies in a New Experimental Model. Circulation 2002;105:2772–8. [PubMed: 12057993]

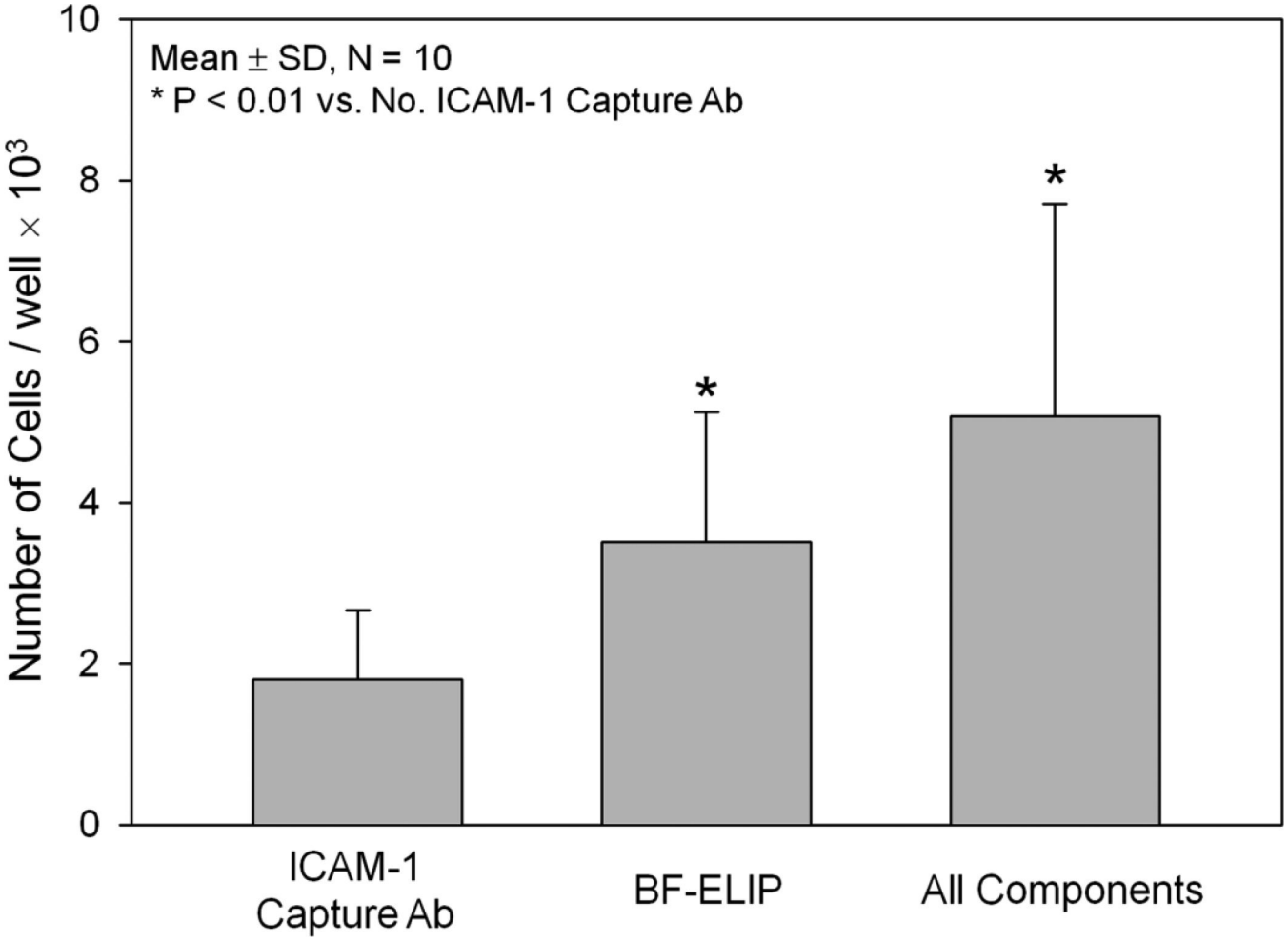

Figure 1.
BF-ELIP bridging of human peripheral CD34+ mononuclear cells to culture wells coated with ICAM-1 protein, utilizing a sandwich ELISA protocol. Adsorbed cells were enumerated after trypsinization by phase contrast microscopy with a hemacytometer.

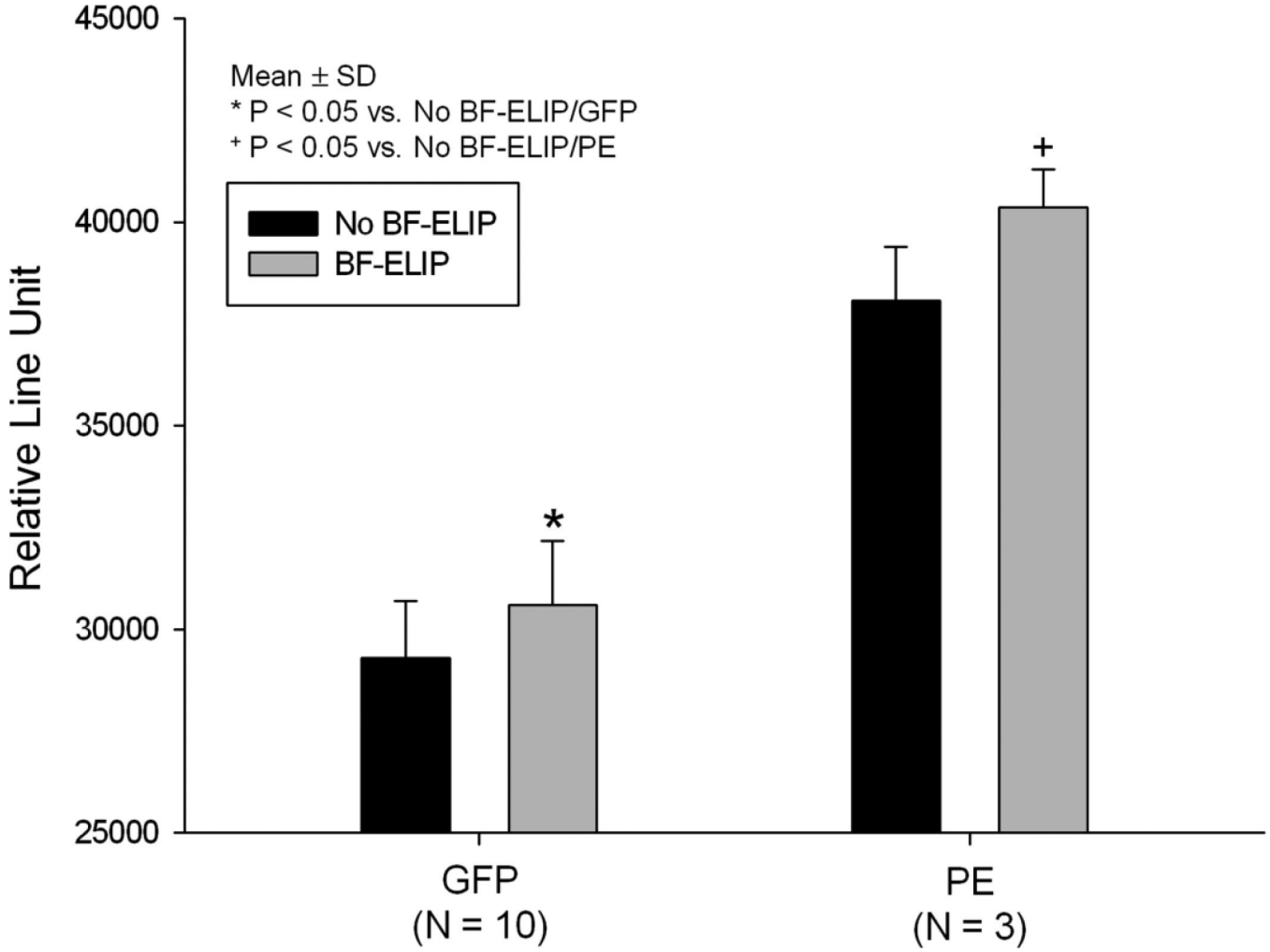

Figure 2.
Ability of BF-ELIP targeted to ICAM-1 and CD34 to bridge GFP-transfected human CD34+ cells, stained with anti-CD34-PE, to HUVEC monolayers in microplate wells. GFP and PE fluorescence is expressed as relative light units.

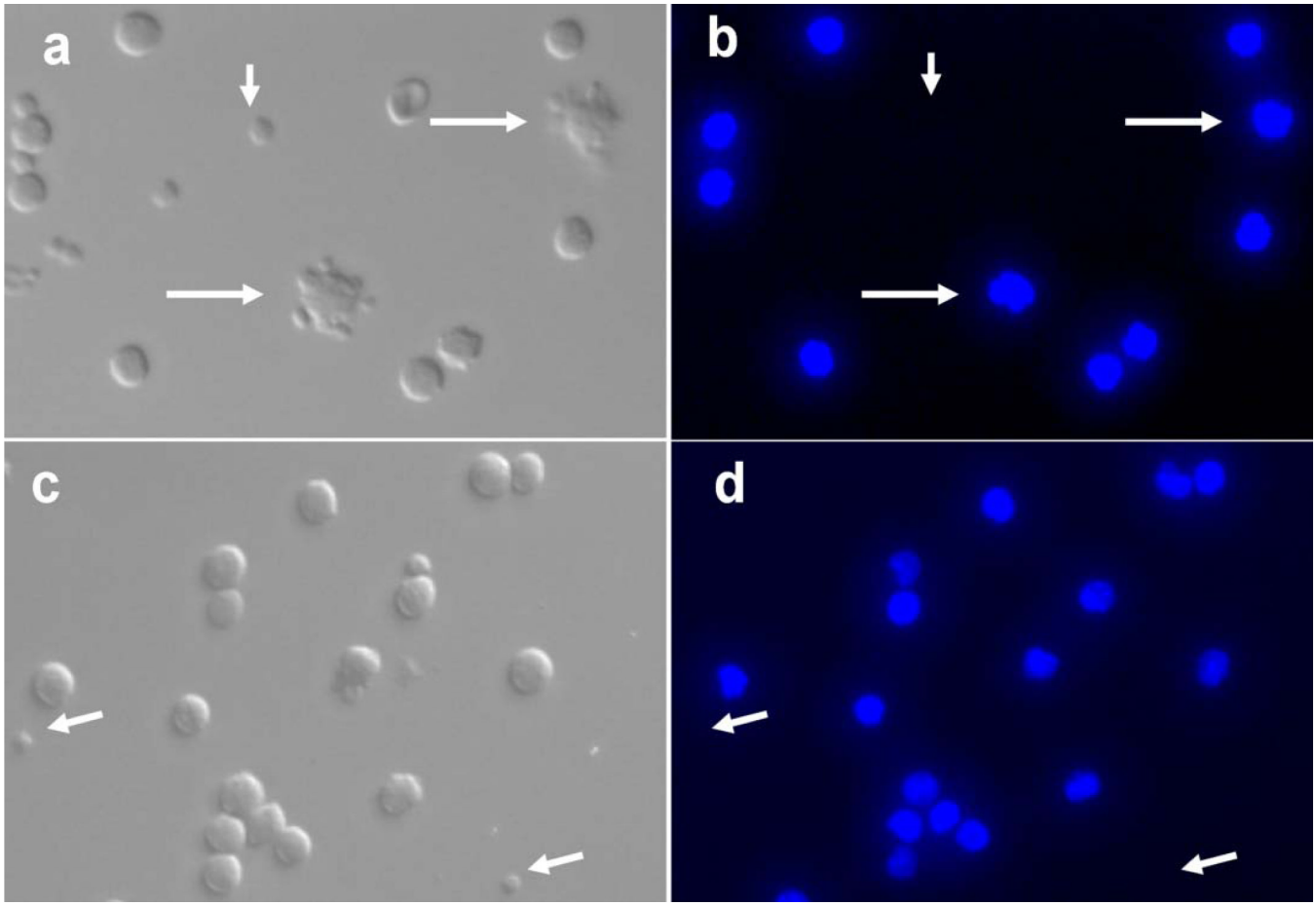

Figure 3.
Microphotographs of BF-ELIP targeted human CD34+ mononuclear cells. (a, c) Bright field images, (b and d) DAPI nuclear fluorescence (blue). Longer arrows point to BF-ELIP-attached stem cells and shorter arrows indicate free BF-ELIP.

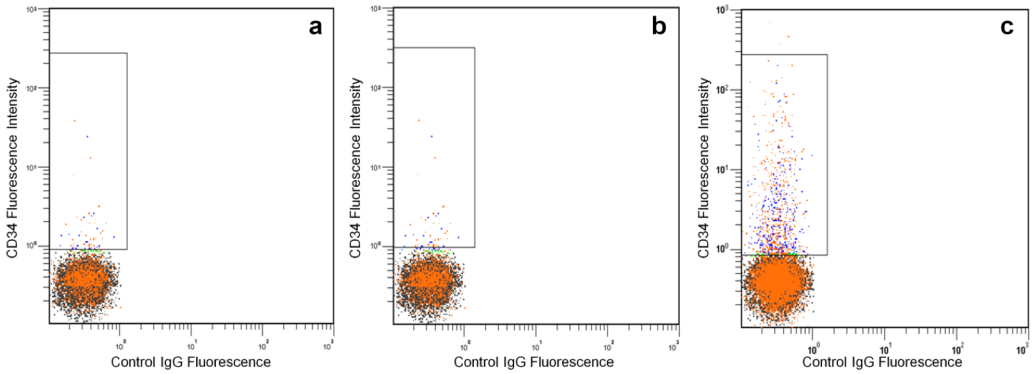

Figure 4.
Flow cytometry of human mononuclear cells incubated with (a) ELIP, (b) IgG-ELIP, and (c) BF-ELIP. PE-conjugated anti-mouse IgG was used to visualize the cells with conjugated ELIP.

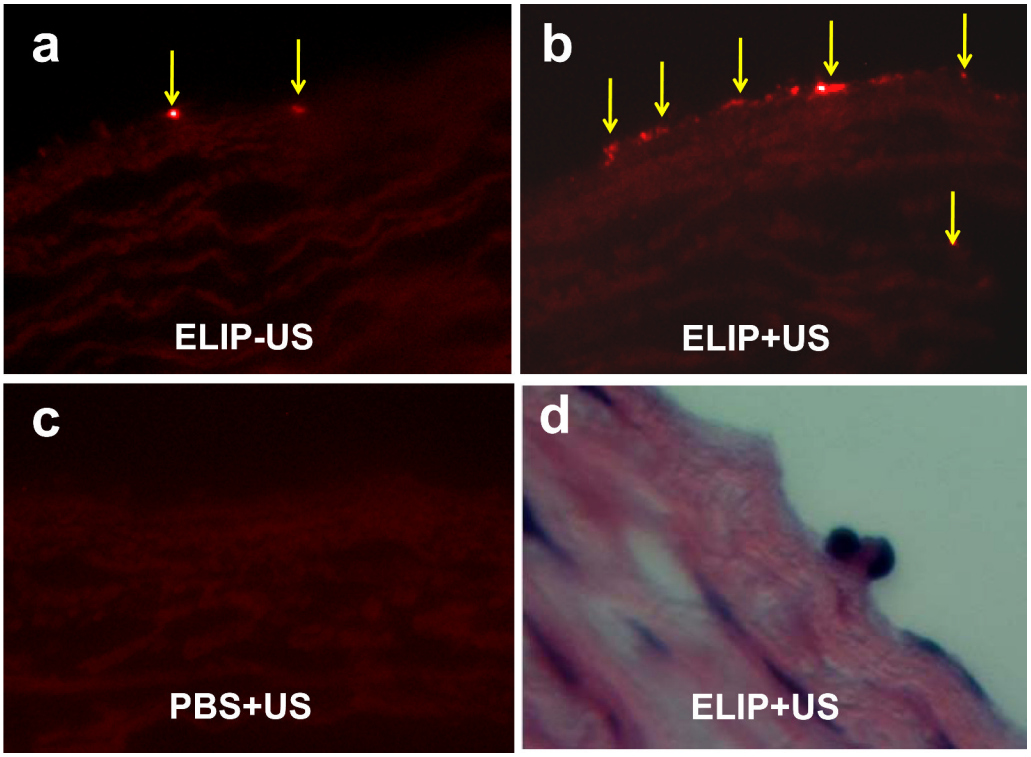

Figure 5.
Fluorescence (a-c) and H&E (d) images of porcine bone marrow CD34+ cells incubated to the lumen of aortic segments preloaded with BF-ELIPs followed by treatment with or without ultrasound. (a) BF-ELIP and CD34+ cells without ultrasound treatment, (b) BF-ELIP and CD34+ cells followed by ultrasound treatment, (c) PBS control and CD34+ cells without ultrasound treatment, and (d) H&E staining of the porcine aortic segment incubated with BF-ELIP and CD34 cells followed by ultrasound treatment. Arrows point to BF-ELIP-stem cell complexes adherent to the aorta.

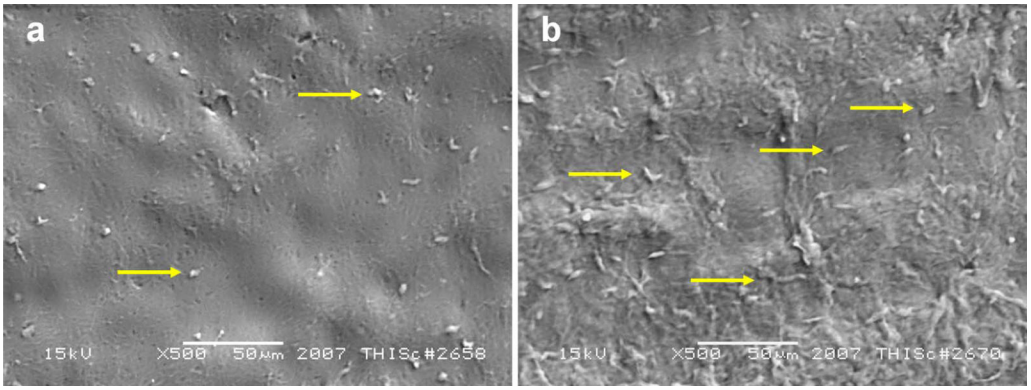

Figure 6.
Scanning electron microscopy of BF-ELIP targeted CD34+ cells adherent to the lumenal surface of porcine aorta with ultrasound treatment. (a) Scattered cell attachment to normal, non-atherosclerotic aortic surface, (b) Increased cell attachment and penetration in region with fatty streaks. Arrows point to BF-ELIP-stem cell complexes adherent to the aorta.

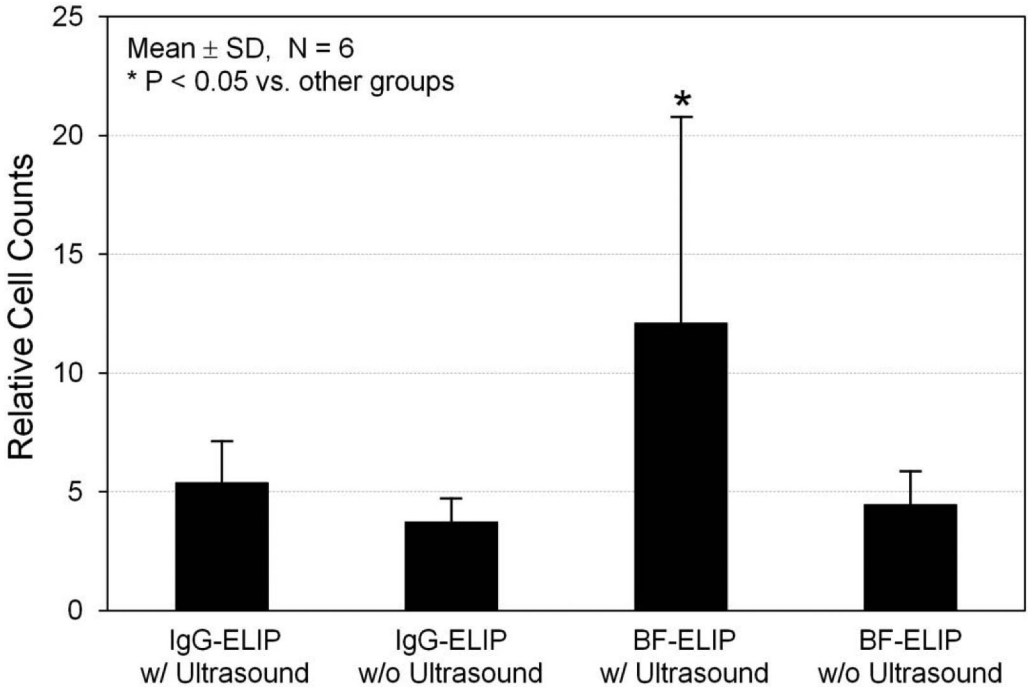

Figure 7.
Quantification of Oil Red O staining of BF-ELIP targeting to the porcine aorta. This demonstrated increased density of Oil Red O staining in the aorta incubated with CD34+ cells with BF-ELIP and ultrasound treatment.